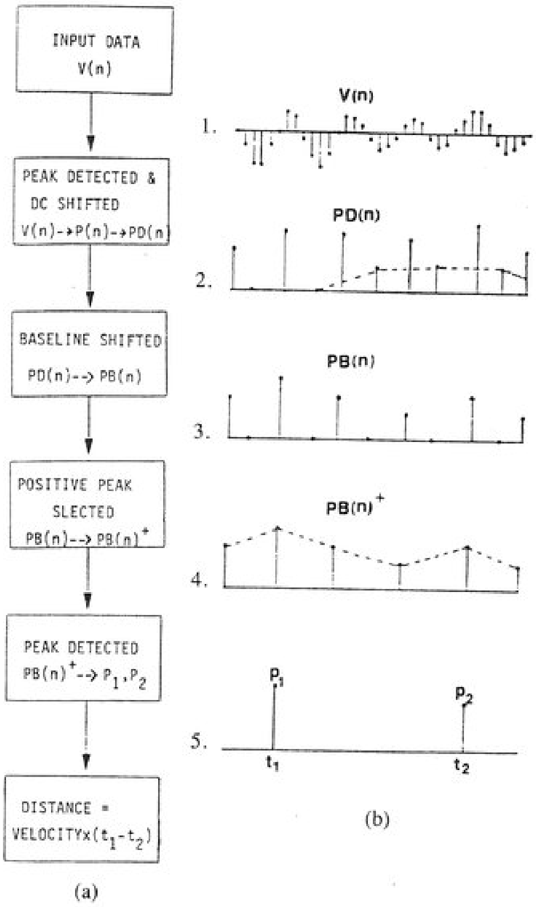

Fig. 3. (a) Flowchart for base-shifted, peak detection program. (b) An illustrative example.

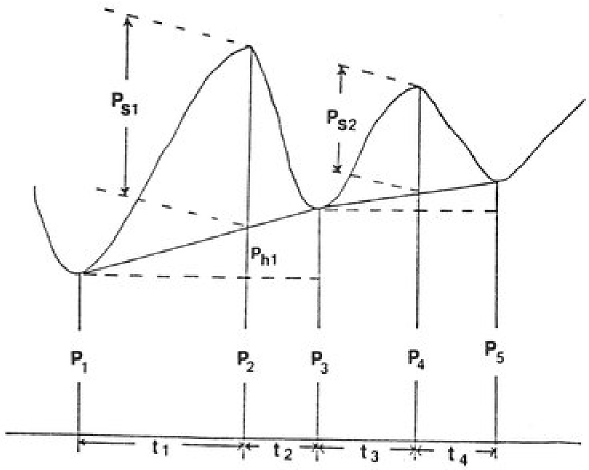

Fig. 4. Baseline independent interval-amplitude analysis.

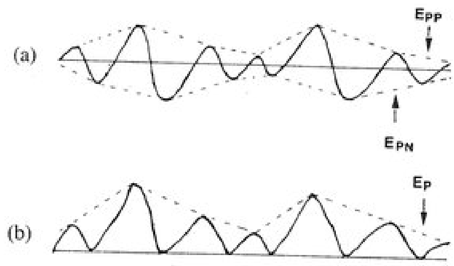

Fig. 5. (a) The envelope of positive peaks (Epp) and negative peaks (Epn). (b) The envelope of peaks (Ep) after the baseline shifting ($Ep = Epp + Epn$).

obtained from input signals by peak detection and dc shifting. A baseline-shifting scheme based on a technique proposed by Fugimori [17] is then applied [part 3 of Fig. 3(b)]. After baseline shifting, the digitized sample points are transformed such that only positive-valued peaks are processed.

Based on the baseline-shifting techniques, the desired Ps_1 and Ps_2 are extracted according to the following algorithms (Fig. 4):

$$Ps_1 = P_2 - \left(P_1 + \frac{|P_3 - P_1| \cdot t_1}{t_1 + t_2}\right) \tag{3}$$

and similarly for Ps_2,

$$Ps_2 = P_4 - \left(P_3 + \frac{|P_5 - P_3| \cdot t_3}{t_3 + t_4}\right). \tag{4}$$

In Fig. 5, the resulting envelope (Ep) of the waveform is the sum of positive peaks (Epp) and negative peaks (Epn) in the original waveform. These were taken as significant features for wave analysis. Finally, the peak detection operator is repeated once for the nonzero peaks to recover the distance between the two tubes [part 5 of Fig. 5(b)].

IV. Results and Summary

The responses for different sizes of tubes and different media are shown in Figs. 6 and 7, respectively. It can be seen easily from Fig. 6 that the larger the tube size, the greater the magnitude of peaks. Also, the magnitude which is expected depends on the medium inside the test tube (Fig. 7). In other words, the higher the energy absorption rate and thermoelastic conversion factor of the medium, the greater the generated pressure.

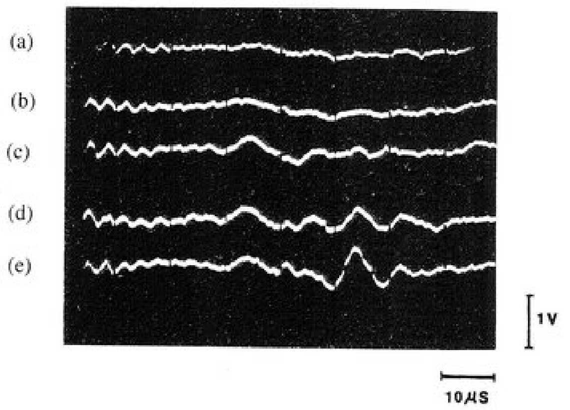

Fig. 6. Thermoelastic responses for individual 2.0 cm diameter tubes filled with different solutions: (a) water, (b) 0.9 percent saline, (c) glycerol, (d) diethylene glycol, (e) glycol. The response from water shows that the effect of glass tube is very small.

The peak detection algorithm was applied to 20 experimental data sets obtained from different combinations of test tubes. Fig. 8 shows that the computer-estimated distance is in close agreement with the actual distance measured from the holder. Slight differences between the actual and estimated data may be due to: 1) low sampling frequency, or 2) poor resolution inherent in the recording system. Moreover, by testing with different distances of separation, it was found that two test objects (diameter = 1.6 cm) could be imaged with spatial resolution of 0.9 cm. When the separation was less than 0.9 cm, the interference between two responses was sufficiently severe to cause the above algorithm to fail.